

DNA strand displacement-based sensor for the detection of miRNA-141 in serum samples

Qiongdan Zhang, Xi Luo, Qingyi Liu, Kang Long, Qiqi Han, Wei Wang,* Bin Li,* Huizhen Wang.*

TCM and Ethnomedicine Innovation & Development International Laboratory, School of Pharmacy, Hunan University of Chinese Medicine, Changsha, China.

Submitted on: 29-Sep-2024, Accepted and Published on: 19-Nov-2024

Article

ABSTRACT

MicroRNA (miRNA) expression is commonly dysregulated in various diseases. Our aim was to develop a simple and sensitive fluorescence-based assay for detecting microRNA-141 (miR-141) activity using DNA strand displacement. In this approach, one strand of the DNA probe (P1) is labeled with a BHQ molecule at its 3'-end, while the complementary strand (P2) is labeled with a FAM molecule at its 5'-end. When P1 and P2 hybridize to form a duplex DNA probe (P1/P2), no fluorescence signal is observed ("off" state). Upon introduction of miR-141 target, the P1/P2 probe undergoes displacement based on the toehold-mediated strand displacement reaction (TMSD), resulting in the formation of a new double-stranded complex between miRNA and P1. This displacement releases a significant amount of single-stranded FAM-labeled nucleotides (P2), resulting in a robust fluorescence signal ("on" state) that enabling target detection. The assay demonstrated high sensitivity for miRNA detection, with a detection limit (LOD) of 0.05 nM. Furthermore, in human serum samples, the sensor exhibited a satisfactory recovery rate ranging from 91.73% to 107.00%, with relative standard deviations (RSD) between 0.24% and 0.69%. These findings underscore its potential as a promising diagnostic tool for cancer.

Keywords: miRNA-141, DNA strand displacement, serum sample

INTRODUCTION

MicroRNAs (miRNAs) are small, endogenous, non-coding RNA molecules typically composed of about 22 bases, crucial for regulating gene expression. They have gained considerable attention in recent years due to their pivotal roles in cellular differentiation, biological development, and the onset and progression of diseases.¹⁻⁴ Extensive molecular biological studies have highlighted the close connections between miRNAs and cancer pathogenesis.⁵⁻¹¹ Specifically, miRNAs influence the expression and structural dynamics of various oncogenes, tumor suppressor genes, and their associated products. Dysregulated miRNA expression is implicated in the initiation, progression, and prognosis of cancer. Hence, developing new miRNA detection technologies that are straightforward, cost-effective, and highly sensitive is imperative. Such innovations could significantly advance cancer research by offering crucial diagnostic insights.

Traditional methods for detecting miRNA include northern blotting,¹²⁻¹³ fluorescent quantitative PCR,¹⁴⁻¹⁶ and microarray technology.¹⁷⁻¹⁹ Northern blotting involves digesting RNA samples with restriction enzymes and separating them via agarose gel electrophoresis to detect miRNA. However, this method is low throughput, time-consuming, prone to degradation, and lacks sensitivity for detecting low abundance miRNA. Fluorescent quantitative PCR converts target miRNA into cDNA via reverse transcription and detects it in real-time using PCR and fluorescence. Despite its advantages, this method suffers from false positives and challenges in primer design. Microarray technology utilizes labeled probes to transcribe RNA samples into labeled cDNAs for detection using oligonucleotides. However, it is costly and less effective for miRNAs with similar sequences. Newer methods include nanomaterial-based [20-23] and fluorescence probe technologies,²⁴⁻²⁸ offering simpler synthesis and lower costs, yet facing issues like complex operation and sequence design challenges.

Compared to traditional methods, DNA-based strand displacement assays offer a simpler, more straightforward approach, eliminating the need for time-consuming procedures. Leveraging this advantage, we have developed a straightforward and sensitive fluorescence-based assay for detecting the activity of miR-141. The platform detects miR-141 by observing

*Corresponding Author: Huizhen Wang, Bin Li, Wei Wang
Email: whuiz0086@163.com (HZ.W.); libin@hnu.edu.cn (B.L.); wangwei402@hotmail.com (W.W.)



URN:NBN:sciencein.cbl.2025.v12.1263
DOI:10.62110/sciencein.cbl.2025.v12.1263
© ScienceIn Publishing
<https://pubs.thesciencein.org/cbl>



fluorescence changes (switching from “off” to “on”) that occur during the strand displacement process. This method enables the analysis of complex biological samples. The recovery rates ranged from 91.73% to 107.00%, with relative standard deviations (RSD) between 0.24% and 0.69%. This innovation is poised to lay a solid foundation for early disease diagnosis and holds promising clinical application potential.

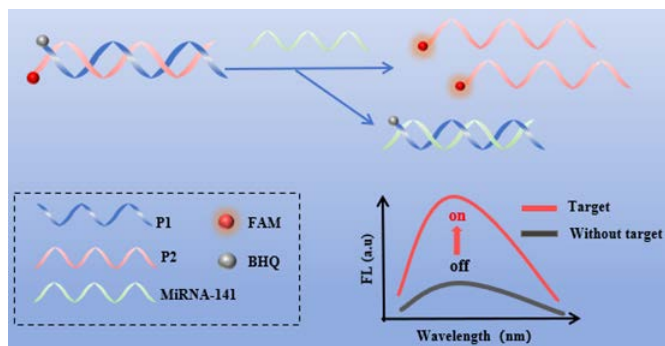


Figure 1. Schematic diagram of the DNA strand displacement sensor.

The design and principle of the method are illustrated in Scheme 1. One strand of the DNA probe (P1) is marked with a BHQ molecule at its 3'-end, while the complementary strand (P2) is labeled with a FAM molecule at its 5'-end. Upon hybridization of P1 and P2 to form a duplex DNA probe (P1/P2), no fluorescence signal is detected (“off” state). Upon the presence of the target miRNA, P2 can be displaced from the P1/P2 probe to create a double-stranded miRNA/P1 complex. Subsequently, large quantities of FAM-labeled single-stranded nucleotides are released, resulting in a robust fluorescence signal (“on” state). The intensity of the fluorescence signal at 525 nm rises with increasing concentrations of the target, indicating improved sensitivity of the method. This enables effective quantitative detection of miRNA.

To assess the feasibility of the DNA strand replacement sensor, we employed polyacrylamide gel electrophoresis (PAGE) alongside fluorescence detection. Initially, we evaluated the chain displacement reaction using fluorescence detection. As shown in Figure 2A, in the presence of target miR-141, the P1/P2 complex disassembles. This results in the displacement of P2 from the P1/P2 probe, forming a double-stranded miRNA/P1 complex that generates significant fluorescence signals (red curve). Conversely, in the absence of miR-141, the P1/P2 complex remains intact, yielding only weak fluorescence (black curve). Further validation was performed using PAGE (Figure 2B), where distinct bands corresponding to P1, P2, and miR-141 are visible in lanes 1, 2, and 3, respectively. Upon incubating equal concentrations of P1 and P2, their individual bands disappear in lane 4, replaced by a new band migrating further, indicative of the formation of the P1/P2 duplex through hybridization. Introducing target miRNA into the P1/P2 duplex solution abolishes the P1/P2 band and generates a broader downstream band (lane 6), consistent with lane 5, indicating a mixture of miRNA and P1. These results confirm that miR-141 effectively initiates the “DNA strand replacement reaction.”

To tailor the DNA strand replacement sensor developed in this study for detecting target miRNA-141 and achieving optimal sensing performance, we optimized two critical experimental parameters: the hybridization ratio and the incubation time of P1 and P2. As depicted in Figure 3A, the fluorescence signal exhibits the widest distinction when the concentration ratio of P1 to P2 reaches 4:1. Hence, the optimal ratio of P1 to P2 was established as 4:1. Furthermore, the incubation times for P1 and P2 were optimized. Increasing the incubation time from 10 to 80 min, the signal peaked at 40 min (Figure 3B). Therefore, 40 min was determined as the optimal incubation time for subsequent miR-141 assays.

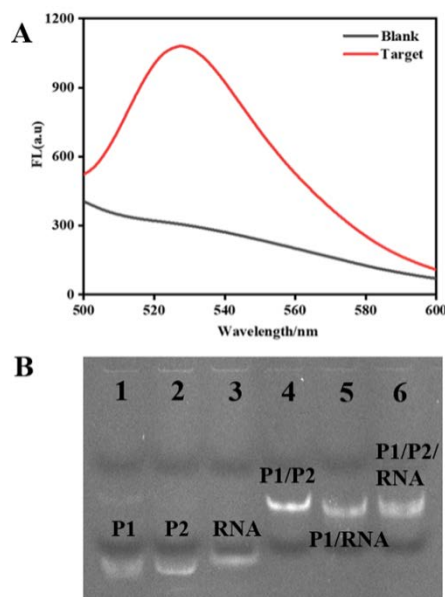


Figure 2. Feasibility of DNA strand displacement sensor. (A) Fluorescence verification of the DNA strand displacement sensor. (B) PAGE characterization of the DNA strand displacement sensor (Lane 1: P1, 1 μ M; Lane 2: P2, 1 μ M; Lane 3: miR-141, 1 μ M; lane 4: P1, 1 μ M and P2, 1 μ M; lane 5: P1, 1 μ M and miR-141, 0.5 μ M; lane 6: P1, 1 μ M, P2, 1 μ M and miR-141, 0.5 μ M).

To validate the superior performance of the DNA strand displacement sensor under optimal conditions, fluorescence emission spectra were measured in response to varying concentrations of the target. Figure 4A illustrates a typical concentration-dependent signal-on response for detecting miR-141 (100–600 nM). The calibration plots demonstrate a linear correlation between fluorescence signals and target concentration. The regression equation for miR-141 (Figure 4B) is expressed as $y = 268.8620 + 0.6632x$ ($R^2 = 0.9930$), where y represents fluorescence intensity at 518 nm, and x denotes target concentration. Based on linear regression, the LOD was calculated as 0.05 nM using the formula $3\sigma/S$ (where σ is the standard deviation of the background signal and S is the slope of the regression line). These findings confirm that the proposed approach enables convenient and sensitive analysis of miR-141.

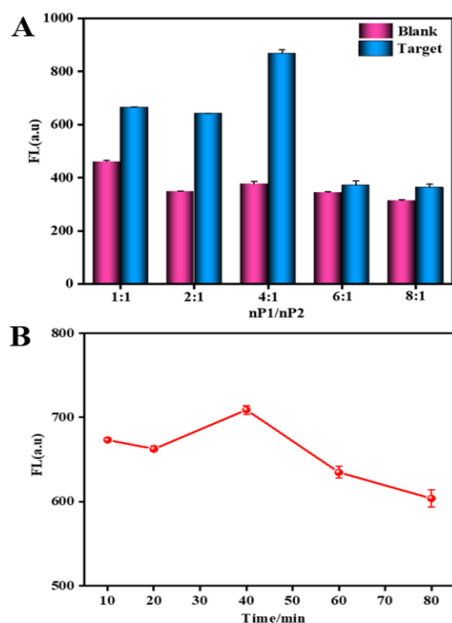


Figure 3. Optimization of experimental conditions. (A) The hybridization ratio of P1 and P2. (B) The incubation time of P1 and P2. Data represent means \pm SD.

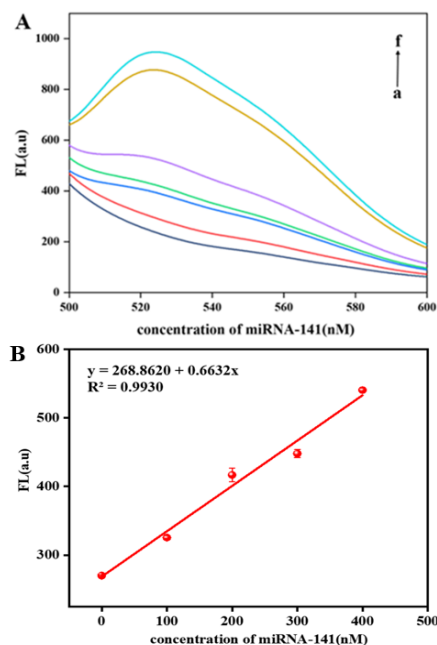


Figure 4. Fluorescence detection of miR-141 using DNA strand displacement sensor. (A) Fluorescence spectra at varying concentrations of miR-141 (a-f: 0, 100, 200, 300, 400, 500, 600 nM). (B) Linear correlation between fluorescence intensity and miR-141 concentration.

We then investigated the specificity of this method in detecting the target miR-141. Given the considerable sequence similarity among miRNA families, we included multiple miRNAs for assessment, such as two non-complementary miRNAs (e.g., miR-21 and miR-122), along with two mismatched sequences of

miR-141 (e.g., 1-mis and 2-mis). As depicted in Figure 5, the signal change for miR-141 was notably higher compared to the mismatched miRNA sequences. These findings indicate that the proposed method exhibits high specificity.

To assess interference resistance, serum was chosen as the biological sample due to its complex composition. When spiked with miR-141 in diluted human serum, recovery rates ranged from 91.73% to 107.00%, with relative standard deviations (RSDs) varying from 0.24% to 0.69%, as detailed in Table 1. These satisfactory findings suggest that the fluorescent biosensor proposed in this study can effectively detect miR-141 in complex biological samples. This method, leveraging DNA strand displacement, holds promise for future applications in early-stage cancer diagnosis in clinical settings.

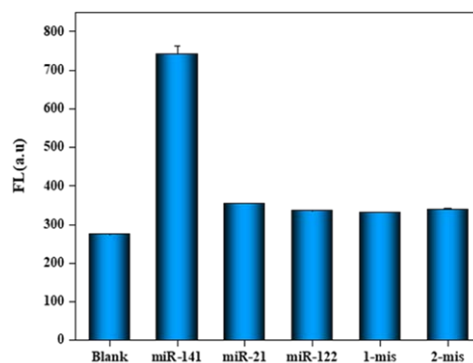


Figure 5. Selectivity for miR-141. From left to right: blank, miR-141, miR-21, miR-122 and 1 nt mismatched of miR-141, 2 nt mismatched of miR-141. Data represent means \pm SD.

Table 1 Recovery results of the biosensor for miR-141 in 100-fold diluted serum (n = 3)

Spiked (nM)	Found (nM)	Recovery (%)	RSD (%)
100	91.73	91.73	0.69
200	214	107	0.24
400	394.12	98.53	0.25

In brief, we have developed a straightforward fluorescence method based on DNA strand displacement to detect miR-141. Our method presents several advantages. Firstly, the method is user-friendly and highly sensitive, enabling straightforward analysis of miR-141 with a LOD of 0.05 nM. Secondly, it is capable of analyzing complex biological samples and is suitable for clinical laboratories. It has successfully quantified miR-141 levels in human serum, achieving recovery rates ranging from 91.73% to 107.00% with RSD between 0.24% and 0.69%. Thirdly, it minimizes reagent and sample usage, thereby lowering analysis costs. We anticipate that this method has substantial potential for advancing biomedical research and clinical diagnostics.

DECLARATION OF COMPETING INTEREST

The authors declare that they have no known competing financial interests or personal relationships that could have appeared to influence the work reported in this paper.

ACKNOWLEDGMENTS

This work was supported in part by the National Natural Science Foundation of China (Grant No. 82304890 and 82074122), and Research Foundation of Education Bureau of Hunan Province (Grant No. 23A0280), and the Changsha Natural Science Foundation (Grant No. Kq2208193), the Opening Funding of Traditional Chinese Medicine and Ethnomedicine Innovation & Development International Laboratory (Grant No. 2022GJSYS04 and 2022GJSYS07) and the Science and Technology Innovation team of Hunan Province (Grant No. 2021RC4064) and the Natural Science Foundation of Hunan Province (Grant No. 2024JJ8128).

SUPPLEMENTARY INFORMATION

The materials, methods and experimental details are available as Supplementary material which can be downloaded from article page online on journal site.

REFERENCES AND NOTES

1. Y. P. Gao, B. Feng, S. Q. Han, et al. The roles of MicroRNA-141 in human cancers: from diagnosis to treatment. *Cell Physiol Biochem*, **2016**, 38(2), 427-448.
2. M. Maleki, A. Golchin, S. Javadi, et al. Role of exosomal miRNA in chemotherapy resistance of colorectal cancer: a systematic review. *Chem Biol Drug Des*, **2023**, 101(5), 1096-1112.
3. M. M. Royam, R. Ramesh, R. Shanker, et al. MiRNA predictors of pancreatic cancer chemotherapeutic response: a systematic review and meta-analysis. *Cancers (Basel)*, **2019**, 11(7), 900.
4. C. Giordano, F. M. Accattatis, L. Gelsomino, et al. MiRNAs in the box: potential diagnostic role for extracellular vesicle-packaged miRNA-27a and miRNA-128 in breast cancer. *Int J Mol Sci*, **2023**, 24(21), 15695.
5. P. R. Jr, M. Yuwanati, S. Sekaran, et al. MiRNA associated with glucose transporters in oral squamous cell carcinoma: a systematic review. *Cureus*, **2023**, 15(9), e46057.
6. A. G. Palacios, A. M. R. Carvajal, A. M. Núñez-Negrillo, et al. MiRNA dysregulation in early breast cancer diagnosis: a systematic review and meta-analysis. *Int J Mol Sci*, **2023**, 24(9), 8270.
7. A. S. Doghish, A. Ismail, H. A. El-Mahdy, et al. A review of the biological role of miRNAs in prostate cancer suppression and progression. *Int J Biol Macromol*, **2022**, 197, 141-156.
8. K. C. Nie, L. Liu, L. Q. Peng, et al. Effects of meranzin hydrate on the lncRNA-miRNA-mRNA regulatory network in the hippocampus of a rat model of depression. *J Mol Neurosci*, **2022**, 72(4), 910-922.
9. B. Alural, S. Genc, S. J. Haggarty. Diagnostic and therapeutic potential of microRNAs in neuropsychiatric disorders: past, present, and future. *Prog Neuropsychopharmacol Biol Psychiatry*, **2017**, 73, 87-103.
10. A. P. Baran, S. S. Głabowska, P. Małkowska, et al. Role of miRNA in melanoma development and progression. *Int J Mol Sci*, **2022**, 24(1), 201.
11. H. A. E. Mahdy, E. G. E. Elsakka, A. A. E. Hussein, et al. MiRNAs role in bladder cancer pathogenesis and targeted therapy: Signaling pathways interplay – A review. *Pathol Res Pract*, **2023**, 242, 154316.
12. C. Martinho, S. L. Gomollon. Detection of microRNAs by northern blot. *Methods Mol Biol*, **2023**, 2630, 47-66.
13. M. R. Green, J. Sambrook. Analysis of RNA by northern blotting. *Cold Spring Harbor Protocols*, **2022**, 22(02), 741.
14. R. N. Wickramasinghe, N. D. S. Goonawardhana, S. P. Premaratne, et al. Quantitative real-time PCR as a novel detection method for micro-RNAs expressed by cervical cancer tissue: a review. *J Biosci Med*, **2021**, 9, 9.
15. S. W. Jung, B. K. Kim, S. J. Lee, et al. Multiplexed on-chip real-time PCR using hydrogel spot array for microRNA profiling of minimal tissue samples. *Sens Actuators B Chem*, **2018**, 1, 228.
16. Q. Y. Ge, F. T. Y. X. Zhou, et al. A universal linker-RT PCR based quantitative method for the detection of circulating miRNAs. *Anal. Methods*, **2014**, 1, 602.
17. F. E. Kanik, I. Celebi, D. Sevenler, et al. Attomolar sensitivity microRNA detection using real-time digital microarrays. *Sci Rep*, **2022**, 12(1), 16220.
18. E. Clancy, M. Burke, V. Arabkari, et al. Amplification-free detection of microRNAs via a rapid microarray-based sandwich assay. *Anal Bioanal Chem*, **2017**, 409(14), 3497-3505.
19. R. Saba, S. A. Booth. Target labelling for the detection and profiling of microRNAs expressed in CNS tissue using microarrays. *BMC Biotechnol*, **2006**, 12(6), 47.
20. B. Mohan, S. D. Kumar, S. Kumar, et al. Nanomaterials for miRNA detection: the hybridization chain reaction strategy. *Sens. Diagn*, **2023**, 2, 78-89.
21. L. H. Ding, H. Y. Liu, L. N. Zhang, et al. Label-free detection of microRNA based on the fluorescence quenching of silicon nanoparticles induced by catalyzed hairpin assembly coupled with hybridization chain reaction. *Sens. Actuators B Chem*, **2017**, 7, 111.
22. J. M. Wang, J. Wen, H. Y. Yan, et al. Recent applications of carbon nanomaterials for microRNA electrochemical sensing. *Chem Asian J*, **2021**, 16(2), 114-128.
23. L. Yu, P. He, Y. C. Xu, et al. Manipulations of DNA four-way junction architecture and DNA modified Fe₃O₄@Au nanomaterials for the detection of miRNA. *Sens. Actuators B Chem*, **2020**, 12, 8015.
24. Z. J. Hu, J. Zhang, Y. M. Li, et al. G-quadruplex-deficient precursor hairpin probes for ultra-low background dual-mode detection of miRNAs. *Talanta*, **2023**, 253, 123954.
25. K. Zhang, Y. Li, S. J. Jiang, et al. Catalytic Assembly of DNAzyme Integrates with Primer Exchange Reaction (CDiPER) for Highly Sensitive Detection of MicroRNA. *ACS Omega*, **2024**, 9(9), 10897-10903.
26. J. M. Xu, X. Cui, L. Wang, et al. DNA-functionalized MOF fluorescent probes for the enzyme-free and pretreatment-free detection of microRNA in serum. *Talanta*, **2024**, 275, 126083.
27. H. M. Zhang, J. Li, H. Huang, et al. Simple, sensitive, and label-free miRNA analysis through strand displacement reaction integrating with G-quadruplex-based signal generation. *J Anal Sci Technol*, **2023**, 46, 947.
28. J. J. Wang, Y. Liu, Z. Ding, et al. The exploration of quantum dot-molecular beacon based MoS₂ fluorescence probing for myeloma-related miRNAs detection. *Bioact Mater*, **2022**, 17, 360-368.